Atmospheric Environment 88 (2014) 370–389

Contents lists available at ScienceDirect

Atmospheric Environment

journal homepage: www.elsevier.com/locate/atmosenv

Ozone formation along the California–Mexican border region during Cal–Mex 2010 field campaign

Guohui Li [a,b,c,*], Naifang Bei [b,d], Miguel Zavala [b], Luisa T. Molina [b,c,*]

[a] Key Laboratory of Aerosol Science and Technology, SKLLQG, Institute of Earth Environment, Chinese Academy of Sciences, Xi'an, China
[b] Molina Center for Energy and the Environment, La Jolla, CA, USA
[c] Massachusetts Institute of Technology, Cambridge, MA, USA
[d] School of Human Settlements and Civil Engineering, Xi'an Jiaotong University, Xi'an, China

HIGHLIGHTS

- Emissions from California contribute more than Baja California to O_3 formation in the border region.
- Biogenic emissions enhance the O_3 level by up to 40 ppb over the mountain region in the afternoon.
- Interactions of California and Baja California emissions decrease afternoon O_3 in the border area.

ARTICLE INFO

Article history:
Received 4 August 2013
Received in revised form
13 November 2013
Accepted 26 November 2013
Available online 16 December 2013

Keywords:
Emissions
Ozone formation
Cal–Mex border
Trans-boundary transport

ABSTRACT

The purpose of this study is to evaluate the ozone (O_3) formation along the California–Mexico border region using the WRF-CHEM model in association with the Cal–Mex 2010 field campaign. Four two-day episodes in 2010 are chosen based on plume transport patterns: 1) May 15–16 (plume north), 2) May 29–30 (plume southwest), 3) June 4–5 (plume east), and 4) June 13–14 (plume southeast). Generally, the predicted O_3 spatial patterns and temporal variations agree well with the observations at the ambient monitoring sites in the San Diego-Tijuana region, but in the Calexico–Mexicali region, the model frequently underestimates the observation. In the San Diego–Tijuana region, the morning anthropogenic precursor emissions in the urbanized coastal plain are carried inland and mixed with the local biogenic emissions during transport, causing the high O_3 level over the mountain region. Biogenic emissions enhance the O_3 concentrations by up to 40 ppb over the mountain region in the afternoon. The factor separation approach is used to evaluate the contributions of trans-boundary transport of emissions from California and Baja California to the O_3 level in the California–Mexico border region. The Baja California emissions play a minor role in the O_3 formation in the San Diego region and do not seem to contribute to the O_3 exceedances in the region, but have large potential to cause O_3 exceedances in the Calexico region. The California emissions can considerably enhance the O_3 level in the Tijuana region. Generally, the California emissions play a more important role than the Baja California emissions on O_3 formation in the border region (within 40 km to the California–Mexico border). On average, the O_3 concentrations in the border region are decreased by 2–4 ppb in the afternoon due to the interactions of emissions from California and Baja California. Further studies need to be conducted to improve the sea breeze simulations in the border region for evaluating O_3 formation.

1. Introduction

Ozone (O_3) is a key trace gas in the atmosphere, not only because it plays a controlling role in the oxidation capacity of the atmosphere, but also because it is one of the most important short-lived greenhouse gases. In addition, high levels of O_3 at the surface are of major environmental concerns due to its detrimental effects on human health and ecosystems, hence O_3 is one of the criteria pollutants regulated by the US Environmental Protection Agency (US EPA) and many countries.

The US and Mexico share a common air basin along the ~200 km border between California and Baja California. The border region embracing the sister cities of San Diego–Tijuana and Calexico–

* Corresponding authors. Massachusetts Institute of Technology, Cambridge, MA, USA.
E-mail addresses: ligh@ieecas.cn (G. Li), ltmolina@mit.edu (L.T. Molina).

1352-2310/$ – see front matter © 2014 Elsevier Ltd. All rights reserved.
http://dx.doi.org/10.1016/j.atmosenv.2013.11.067

Mexicali has become an environmentally stressed area due to growing population, expanding industries, increasing transportation activity, older vehicles on roads, and unplanned city expansions (Shi et al., 2009). For example, the sister-city pair of San Diego–Tijuana exceeded the US National Ambient Air Quality Standard (NAAQS) maximum 8-h average O_3 of 80 ppb 15 days per year on average between 2001 and 2005 (EPA, 2008). The US NAAQS for daily maximum 8-h average O_3 has been decreased recently to 75 ppb, and is likely to be lowered further in future regulatory reviews of its direct impacts on human health (EPA, 2008). Considering the increasingly stringent air quality standards, further studies are imperative to verify the O_3 and other pollutants formation from both natural and anthropogenic emission sources, together with international transboundary transport of pollutants or their precursors along the California–Mexico border region.

Several studies on O_3 formation along the border region have been performed based on field studies and chemical transport model simulations. Through analysis of O_3 episode during the San Diego Air Quality Study, Bigler-Engler and Brown (1995) pointed out that high O_3 concentrations in the San Diego Air Basin are caused not only from local emissions, but also the transport of O_3 and precursors from Los Angeles area. Using aircraft measurements over the San Diego metropolitan area, Luria et al. (2005) demonstrated that the high O_3 plume during mid-day hours in the lower level of the planetary boundary layer (PBL) is produced in the downwind region of the high traffic area in the vicinity of downtown area. Using the process analysis tools of the Community Multiscale Air Quality (CMAQ) modeling system together with back-trajectory analysis, Shi et al. (2009) showed that high-altitude regional transport followed by fumigation contributes significantly to the O_3 levels in San Diego. They have also indicated that the high levels of O_3 in Imperial Valley are influenced by transport from the coastal area of southern California and Mexico. Wang et al. (2009) used a global chemical transport model (CTM) to verify the effects of anthropogenic emissions from Canada, Mexico, and outside North America on daily maximum 8-h average O_3 concentrations in US surface air. They found that exceedances of the 75 ppb US NAAQS in southern California are often associated with Mexican pollution enhancements in excess of 10 ppb. Huang et al. (2011) highlighted the importance of local emissions and long-range transport to the O_3 levels in the South Coast of California.

During May 15 — June 30, 2010, an intensive field campaign along the California–Mexico border region (referred to as Cal–Mex 2010 field campaign) was conducted, in order to characterize the sources and processing of emissions in the border region to better understand their transport and impacts on regional air quality and climate, and to support the design and implementation of emission control strategies at local, regional and trans-boundary scales (Bei et al., 2013). A comprehensive data set was obtained during the campaign, including highly time-resolved ambient gas phase species and aerosols. The data set provides a good opportunity to investigate O_3 formation along the border region. The purpose of the present study is to evaluate the O_3 formation from anthropogenic and natural sources, and the interaction of emissions from California and Mexico. The WRF-CHEM model, the model configuration and the analysis method are described in Section 2. Results of the modeling experiments and comparisons are presented in Section 3, and the Conclusions are given in Section 4.

2. Model and method

2.1. WRF-CHEM model

The model used in this work has been described in previous studies (Li et al., 2010, 2011a, b; 2012). Briefly, a specific version of the WRF-CHEM model (Grell et al., 2005) is utilized to evaluate the O_3 formation along the California–Mexico border region, which is developed by Li et al. (2010) at the Molina Center for Energy and the Environment (MCE2), with a new flexible gas phase chemical module and the CMAQ (version 4.6) aerosol module developed by US EPA.

The inorganic aerosols are simulated in the WRF-CHEM model using ISORROPIA Version 1.7 (http://nenes.eas.gatech.edu/ISORROPIA/). The secondary organic aerosol (SOA) formation is simulated using a non-traditional SOA model including the volatility basis-set modeling method in which primary organic components are assumed to be semi-volatile and photochemically reactive and are distributed in logarithmically spaced volatility bins. Detailed description about the volatility basis-set approach can be found in Li et al. (2011a).

2.2. Model configuration

Four two-day episodes in 2010 are selected in the present study based on Bei et al. (2013): 1) May 15–16 (plume north), 2) May 29–30 (plume southwest), 3) June 4–5 (plume east), and 4) June 13–14 (plume southeast). The WRF-CHEM model is configured with one grid with spacing of 2 km (151 × 101 grid points) centered at 32.75°N and 116.25°E (Fig. 1). Thirty-five vertical levels are used in a stretched vertical grid with spacing ranging from 30 m near the surface, to 500 m at 2.5 km and 1 km above 14 km. The model employs Lin et al. (1983) microphysics scheme, Yonsei University PBL scheme (Noh et al., 2001), Noah land-surface model (Chen and Dudia, 2001), the longwave radiation parameterization (Mlawer et al., 1997), and the shortwave radiation parameterization (Dudia, 1989). The meteorological initial and boundary conditions are from NCEP 1° × 1° reanalysis data. The chemical initial and boundary conditions are interpolated from MOZART 6-h output.

2.3. Emission inventory

A model-ready version of the official emissions inventories (SPARC99) for Tijuana and Mexicali has been developed at MCE2. The most recent emissions inventories for Tijuana and Mexicali were published in 2010 and 2009, respectively, and correspond to the 2005 base year. Both inventories include annual emissions of NO_x, SO_2, Volatile Organic Compounds (VOCs), CO, particulate matter (PM_{10} and $PM_{2.5}$, with aerodynamic diameter less than 10 and 2.5 μm, respectively), NH_3 and CH_4 for point, area, on-road, off-road, and biogenic sources in these municipalities.

The conversion of the Mexican emissions inventories into model-ready datasets involves the development of a Geographical Information System (GIS) platform for the creation of the spatial distributions, the temporal emissions distributions, as well as the chemical speciation (SAPRC99) of VOCs and PM for individual sources. For this, we have requested and obtained from the Mexican government agencies the raw datasets used for the development of the official emissions inventories. Thus, the specific location is used for the spatial distributions of industries and area sources whenever the exact coordinates are available in the inventories raw datasets. This includes all the registered Federal and State industries in the Mexican inventories as well as other point sources that can be easily geo-referenced (e.g., gas fuel stations). For area emission sources that are linked to production processes (e.g., bakeries, dry cleaning, etc.), specific proxies are also used when available from the 2010 Mexican National Economic Census. Other population-based emission sources (e.g., solvent consumption, domestic cooking, etc.) are distributed using population density proxies. Mobile sources are distributed using the road-infrastructure proxies. All the geo-referenced sources are mapped

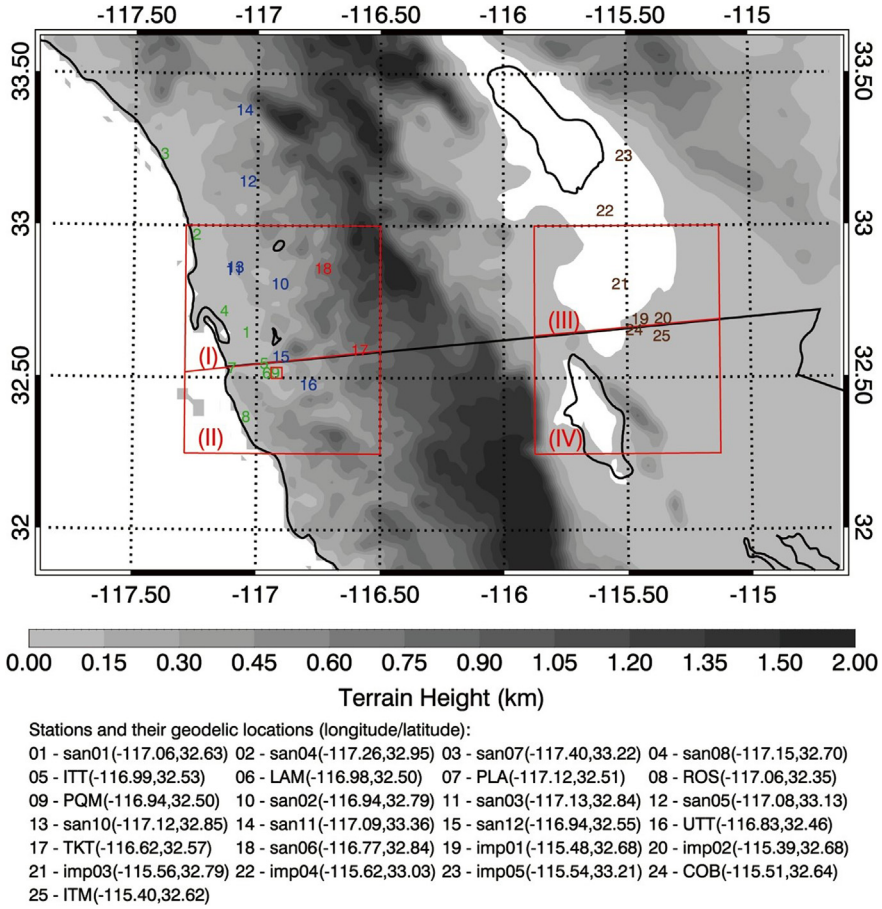

Fig. 1. WRF-CHEM simulation domain and geographic distributions of surface monitoring stations in the California–Mexico border region. The green, blue, and red numbers represent the O_3 and NO_2 monitoring sites with altitude less than 100 m, between 100 and 500 m, and more than 500 m, respectively in the San Diego–Tijuana region. The brown numbers represent O_3 monitoring sites in the Calexico–Mexicali region. The red square is the supersite Parque Morelos (PQM) in Tijuana. Four areas surrounded by trapezia are defined for the factor separation approach: (I) San Diego, (II) Tijuana, (III) Calexico, and (IV) Mexicali and their surrounding areas. (For interpretation of the references to color in this figure legend, the reader is referred to the web version of this article.)

into a 2-km resolution grid. The model-ready emissions input fields for California are directly obtained from the publicly available databases from California Air Resources Board (CARB). Since the model-ready CARB emissions inventory has a resolution of 4 km, we have used the population distribution to interpolate the California emissions into a 2-km resolution grid that is compatible with the Mexican inventories. Additionally, the biogenic emissions are calculated on-line with the WRF-CHEM model using the MEGAN model (Guenther et al., 2006).

2.4. Factor separation technique

Regional O_3 formation is a complicated nonlinear process in which O_3 precursors from natural and anthropogenic emission sources and transport react chemically. Model studies are necessary to evaluate the contribution from different sources to the regional O_3 level for O_3 control strategies. However, it is not straightforward to evaluate the impacts of several different factors in a nonlinear process. The total impact of one factor in the presence of others can be separated into contributions from the factor and that from the interactions of all those factors. We have applied the factor separation approach (FSA) proposed by Stein and Alpert (1993) to decompose the impact of a factor from its interaction with the other factors.

Considering there are two factors X and Y that influence the O_3 formation and also interact with each other, we denote f_{XY}, f_X, f_Y, and f_0 as the simulation results including both factors X and Y, factor X alone, factor Y alone, and none of the two factors, respectively. The pure impacts (denoted by a prime) of factor X and Y are respectively expressed as:

$$f_X^{'} = f_X - f_0$$

$$f_Y^{'} = f_Y - f_0$$

The simulation including both factors X and Y is given by:

$$f_{XY} = f_0 + f_X^{'} + f_Y^{'} + f_{XY}^{'}$$

Then the interactions between A and B is expressed as:

$$f_{XY}^{'} = f_{XY} - f_0 - f_X^{'} - f_Y^{'} = f_{XY} - (f_X - f_0) - (f_Y - f_0) - f_0$$
$$= f_{XY} - f_X - f_Y + f_0$$

This shows that the verification of the contribution from the two factors, and from their possible interactions, needs four simulations, namely, f_{XY}, f_X, f_Y, and f_0.

2.5. Statistical methods for comparisons

In order to evaluate the performance of the WRF-CHEM model in simulating gas-phase species against measurements, the mean

bias (MB), the root mean square error (RMSE), and R squared (R^2) are used in the study.

$$\mathrm{MB} = \frac{1}{N}\sum_{i=1}^{N}(P_i - O_i)$$

$$\mathrm{RMSE} = \left[\frac{1}{N}\sum_{i=1}^{N}(P_i - O_i)^2\right]^{\frac{1}{2}}$$

$$R^2 = \frac{\left[\sum_{i=1}^{N}(P_i - \overline{P})\left(O_i - \overline{O}\right)\right]^2}{\sum_{i=1}^{N}(P_i - \overline{P})^2\sum_{i=1}^{N}\left(O_i - \overline{O}\right)^2}$$

where P_i and O_i are the predicted and observed pollutant concentration, respectively. N is the total number of the predictions used for comparisons, and $\overline{P}$ and $\overline{O}$ denotes the average of the prediction and observation, respectively.

3. Results

3.1. Model performance

Bei et al. (2013) employed the WRF-FLEXPART simulations with particles released in Tijuana in the morning and classified four representative plume transport patterns during Cal–Mex 2010: "plume southeast", "plume southwest", "plume east" and "plume north". In the present study, we choose four 2-day episodes corresponding to the four plume transport patterns to evaluate the O_3 formation along the California–Mexico border region.

In San Diego–Tijuana, the terrain generally increases from sea level along the coast to over 1200 m above sea level inland from the west to east, with isolated peaks of more than 2100 m. The meteorology in the region is determined by the interaction of the semi-permanent Pacific high and the coastal marine environment. The sea breeze intrudes as far inland as the mountain crests. In general, elevated O_3 levels can be formed when morning precursor emissions in the urbanized coastal region chemically react as they are carried inland toward the foothills (Bigler-Engler and Brown, 1995).

For the discussion convenience, the reference run is defined as the WRF-CHEM model simulation with both the anthropogenic and biogenic emissions. Simulated near-surface O_3 concentrations in the reference run are compared with the observations in the California–Mexico border region. Due to the predominant impact of meteorological conditions on air pollution simulations (Bei et al., 2008, 2010), in Fig. 2, we show the spatial distributions of calculated and observed near-surface O_3 concentrations at 1400 Local Time (LT) during the four episodes along with the simulated wind fields in the border region.

Generally, the predicted O_3 spatial patterns are in good agreement with the observations at the ambient monitoring sites in the San Diego–Tijuana region during the four episodes. For example, the model successfully reproduces the observed increasing O_3 concentrations from the coast to the mountain area, but the model sometimes overestimates the observation in the coastal region, which perhaps is caused by the simulated weak on-shore winds that fail to carry the plume formed over sea and coastal emission source regions efficiently. During the plume north episode (May 16–17), in Tijuana, the on-shore southwest winds carry the pollutants out of the region, so the simulated O_3 level is low, which agrees reasonably well with the observations. On May 16, high O_3 concentrations exceeding 60 ppb in San Diego are formed due to the convergence of on-shore westerly winds and inland easterly winds. However, on May 17, the pollutants are carried inland across the mountains by the strong on-shore westerly winds, and the O_3 concentrations in San Diego are not high. During the rest of three episodes, the high O_3 levels are primarily formed over the mountain area where the on-shore westerly winds encounter the inland easterly winds. On May 29 and 30 (plume southwest), the inland northeast winds are so strong that the formed plumes are even forced back to the southwest or the emission source region. The most polluted event occurs on June 4 and 5 (plume east), with the maximal O_3 concentration exceeding 100 ppb over the mountain area. The northwest on-shore winds on June 13 and 14 (plume southeast) in Tijuana bring the precursors emitted in the urban area to the southeast of the city.

In the Calexico–Mexicali region, the model performs well in simulating the O_3 distribution during the plume north and east episodes, but substantially underestimates the observed O_3 concentrations on plume southwest (May 29) and southeast (June 13) episodes. Model performance is generally influenced by uncertainties in the emission inventories and meteorological fields. Since the emission inventories work reasonably well for the O_3 distribution simulations except for these two days, the uncertainties of the model simulated meteorological fields become the dominant reason for the model biases. Previous studies have shown that meteorological conditions play a key role in determining the accumulation or dispersion of pollutants and significantly influence the O_3 simulation in CTMs (Bei et al., 2008, 2010). Fig. 3 presents the wind fields along with the CO distribution at 0700 and 1000 LT on May 29 and June 13. The consistent northwest winds dominate in the urban areas in the morning in the Calexico–Mexicali region, and transport the pollutants (indicated by CO) to the southeast of Mexicali. The efficient dispersion does not facilitate the accumulation of pollutants and the O_3 formation in the region, causing the model underestimation of O_3 concentrations.

Fig. 4 presents the diurnal variations of simulated and observed near-surface O_3 concentrations averaged over the ambient monitoring sites for the four episodes in San Diego–Tijuana. Generally, the model reproduces the observed temporal variations of O_3 concentrations reasonably well. For example, the model successfully predicts the noontime O_3 peaks due to photochemical activities and the low nighttime O_3 caused by the titration of emitted NO. The nighttime simulated O_3 frequently deviates considerably from the observations, except during the plume east episode, due to difficulties in modeling the night-time meteorological fields and the complexity of the nocturnal chemistry (Li et al., 2007). In Calexico–Mexicali (Fig. 5), the model often underestimates the observation during daytime due to the biases of simulated meteorological fields that do not facilitate the accumulation of pollutants.

Compared with the measurements, the simulated NO_2 pattern is not as good as those for O_3, due to the short lifetime of NO_2 and spatial heterogeneity of its emissions (Fig. 6). In general, the model reasonably reproduces the observed high NO_2 concentrations in and around the urban area of Tijuana, but frequently overestimates the observation in and around the urban area of San Diego. Because of the limited observation sites in the Calexico–Mexicali region, we only show the diurnal variations of simulated and observed near-surface NO_2 concentrations averaged over the ambient monitoring sites in San Diego–Tijuana in Fig. 7. Although the model captures well the observed variation of NO_2 concentrations, it often underestimates or overestimates the observation during nighttime in San Diego–Tijuana, which is perhaps caused by the uncertainties of simulated meteorological fields or the emission inventory.

Table 1 shows the MB, RMSE, and R^2 for each station individually for O_3 and NO_2 to illustrate the model performance and the importance of biases in the WRF-CHEM model. The model generally performs well in simulating temporal variations of O_3

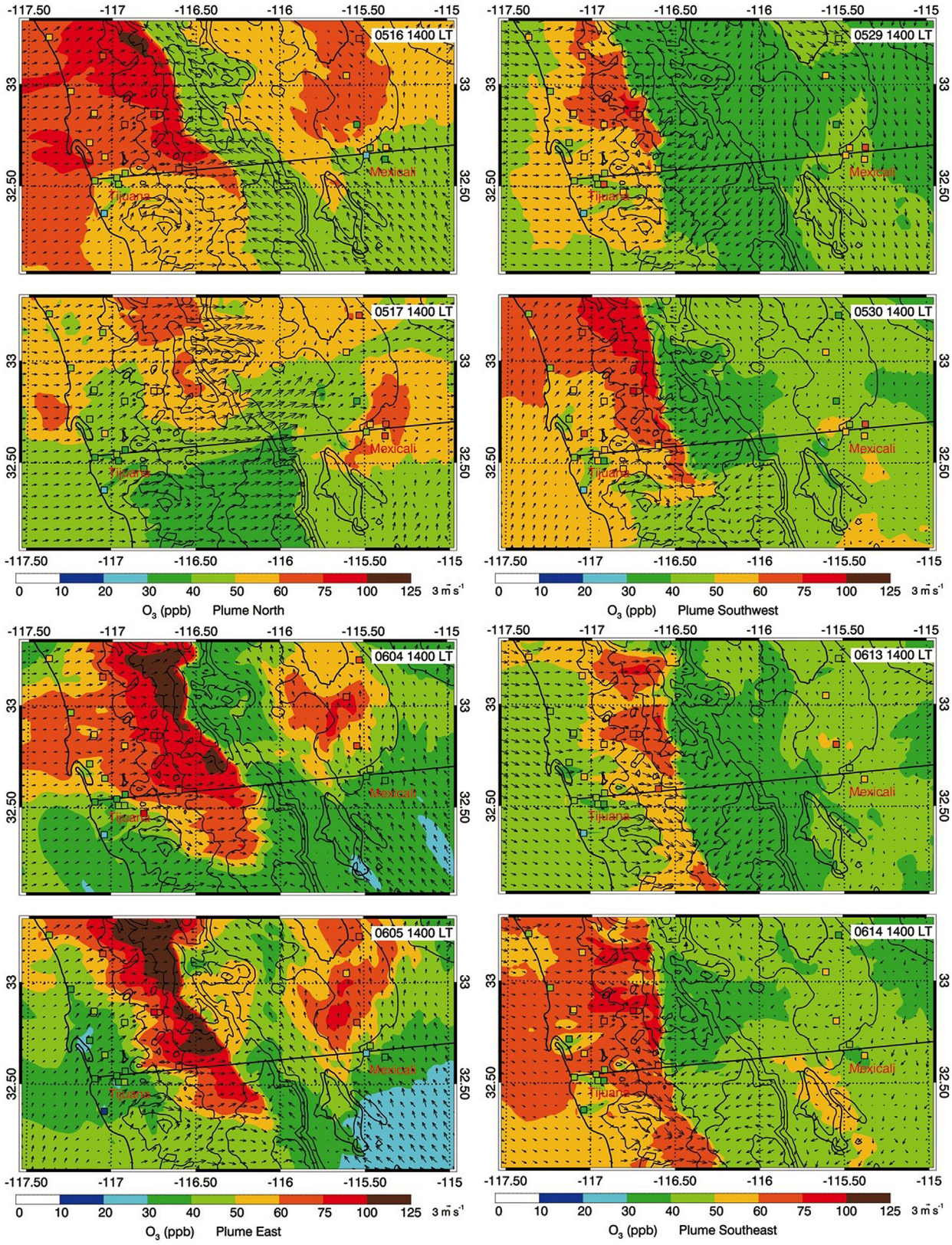

Fig. 2. Pattern comparison of simulated vs. observed near-surface O_3 at 1400 LT during the four selected episodes. Colored squares: O_3 observations; color contour: O_3 simulations; black arrows: simulated surface winds. (For interpretation of the references to color in this figure legend, the reader is referred to the web version of this article.)

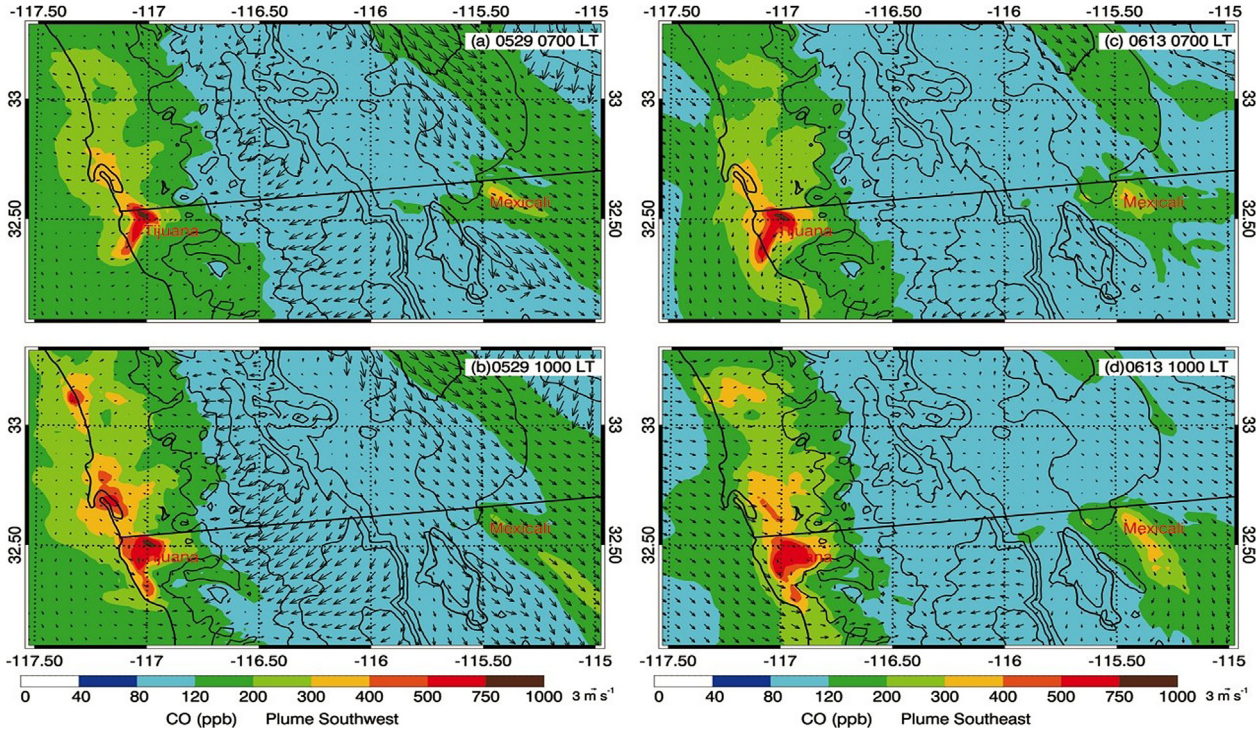

Fig. 3. Simulated near-surface winds and CO at 0700 and 1000 LT on May 29 and June 13. Color contour: CO simulations; black arrows: simulated surface winds. (For interpretation of the references to color in this figure legend, the reader is referred to the web version of this article.)

concentrations at each station, with MB ranging from −14.3 ppb to 13.5 ppb, R^2 ranging from 0.20 to 0.79, and RMSE ranging from 7.1 to 22.0. The R^2 at most of sites is over 0.40, indicating good correlation of simulations with observations on those sites. However, the model does not yield good NO_2 simulations according to the statistical analysis in Table 1, with R^2 less than 0.38. Bei et al. (2012) have highlighted that uncertainties in simulated meteorological fields significantly impact the simulations of CTMs when the comparison is made on a single site, therefore the biases in meteorological fields simulations might constitute one of the possible reasons for the gap between model and observations of NO_2 concentrations at each station.

The sea breeze in San Diego–Tijuana plays an important role in the transportation of emissions in the urbanized coastal region.

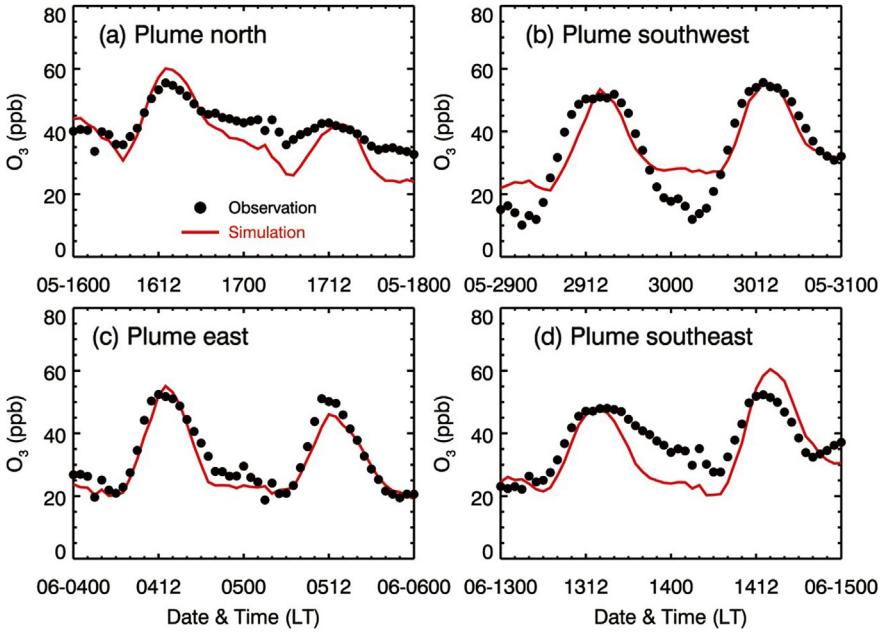

Fig. 4. Comparison of measured (black dots) and simulated (red line) diurnal profiles of near-surface hourly O_3 averaged over all monitoring sites in the San Diego–Tijuana region during the four selected episodes. (For interpretation of the references to color in this figure legend, the reader is referred to the web version of this article.)

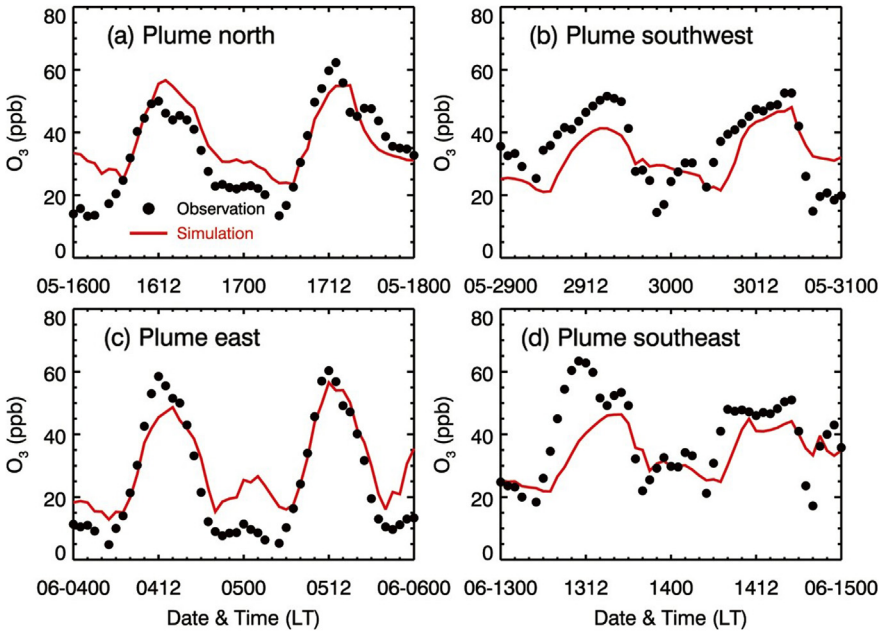

Fig. 5. Same as Fig. 4, but in the Calexico–Mexicali region.

Wang et al. (2013) have discussed the effect of sea breeze on the smoke transport over the Southeast Asian maritime continent. Following the method of Wang et al. (2013), Fig. 8 illustrates the diurnal profiles of the simulated and observed surface wind speed and direction at PMQ (see Fig. 1), and simulated surface winds and CO distributions along the California–Mexico border region at 0200, 0800, 1400, and 2200 LT on May 29. The WRF-CHEM model reasonably simulates the variation of the wind speed and direction at PQM, particularly the abrupt change of the wind direction, but it often overestimates the wind speed by 1–2 m s^{-1}, and the simulated wind direction change between 2100 and 2300 LT is delayed against the measurement. The surface winds in the coastal region are weak and off-shore at 0200 LT, and become calm at 0800 LT, causing accumulation of emitted precursors (indicated by CO). At 1400 LT, the on-shore sea breeze is dominant in the coastal region and transports the emitted precursors to the high-altitude region. Convergence is formed over the region where the onshore sea breeze encounters the inland easterly wind. At 2000 LT, the sea breeze decays and the surface winds are disordered in the coastal region. The convergence caused by the sea breeze facilitates accumulation of pollutants, leading to high O_3 formation over the high-altitude region. Furthermore, considering the model performance in simulating O_3 and NO_2 clearly depends on local time and aerosols and other pollutants co-vary with sea breeze, it is possible that aerosols (such as sea salt) could impact O_3 and NO_2 through heterogeneous chemistry. Laboratory and field studies have demonstrated that nitryl chloride ($ClNO_2$) is produced efficiently from the heterogeneous reaction of dinitrogen pentoxide (N_2O_5) on sea salt and accumulate at night (Osthoff et al., 2008). $ClNO_2$ can be photolyzed after sunrise to produce chlorine atoms, enhancing oxidation of VOCs and accelerating photochemical O_3 production. However, the heterogeneous reaction of $ClNO_2$ on sea salt is not included in the WRF-CHEM model and further studies need to be performed to evaluate the contribution of the reaction on O_3 formation in the coastal region.

The sea breeze transport causes the gradient of O_3 distributions from the coastal to mountain area in the San Diego–Tijuana region. Simulated O_3 distributions have been compared with the observations at monitoring sites, but the site measurements are still limited and discrete. In contrast, aircraft measurements can provide detailed spatial and temporal information on O_3 distribution and variation. Luria et al. (2005) have performed air-quality samplings using an aircraft over the San Diego metropolitan area during July 2003 to evaluate the impact of offshore pollution sources on the air quality in this region. They found that, during most flights, the pollution cloud with high O_3 level during the mid-day hours in the lower level of the PBL is formed in the downwind region of the high traffic area in the vicinity of downtown area, which is consistent with the WRF-CHEM simulations. In addition, the marine layer clouds formed over the adjacent ocean waters can be advected by the sea breeze over San Diego–Tijuana in the morning. The clouds scatter incoming solar radiation and reduce photolysis rates in the PBL, decreasing the observed O_3 and NO_2 concentrations at monitoring sites. However, the model generally cannot resolve adequately the marine layer cloud coverage, which is one of the possible reasons for the model biases in simulating O_3 and NO_2.

During daytime, the predicted pattern and variation of O_3 and NO_2 are generally in good agreement with the corresponding measurements, indicating that the model simulates reasonably well the meteorological fields and the emissions used are also reasonable.

3.2. O_3 sensitivity to emission changes

High O_3 formation in the urban center and its downwind region is caused by its precursors of anthropogenically emitted VOCs and NO_x, as well as biogenic VOCs (Chameides et al., 1988; Li et al., 2007). Numerous studies have been conducted to develop an effective O_3 control strategy by reducing O_3 precursor emissions; thus it is important to understand the nonlinear relationship between O_3 and its precursors. The regime of O_3 production along the California–Mexico border regions is investigated by the sensitivity studies of O_3 formation through reducing anthropogenic VOCs (AVOCs) or NO_x emissions by 50%. Fig. 9 presents the averaged O_3 change with a 50% reduction in NO_x emissions

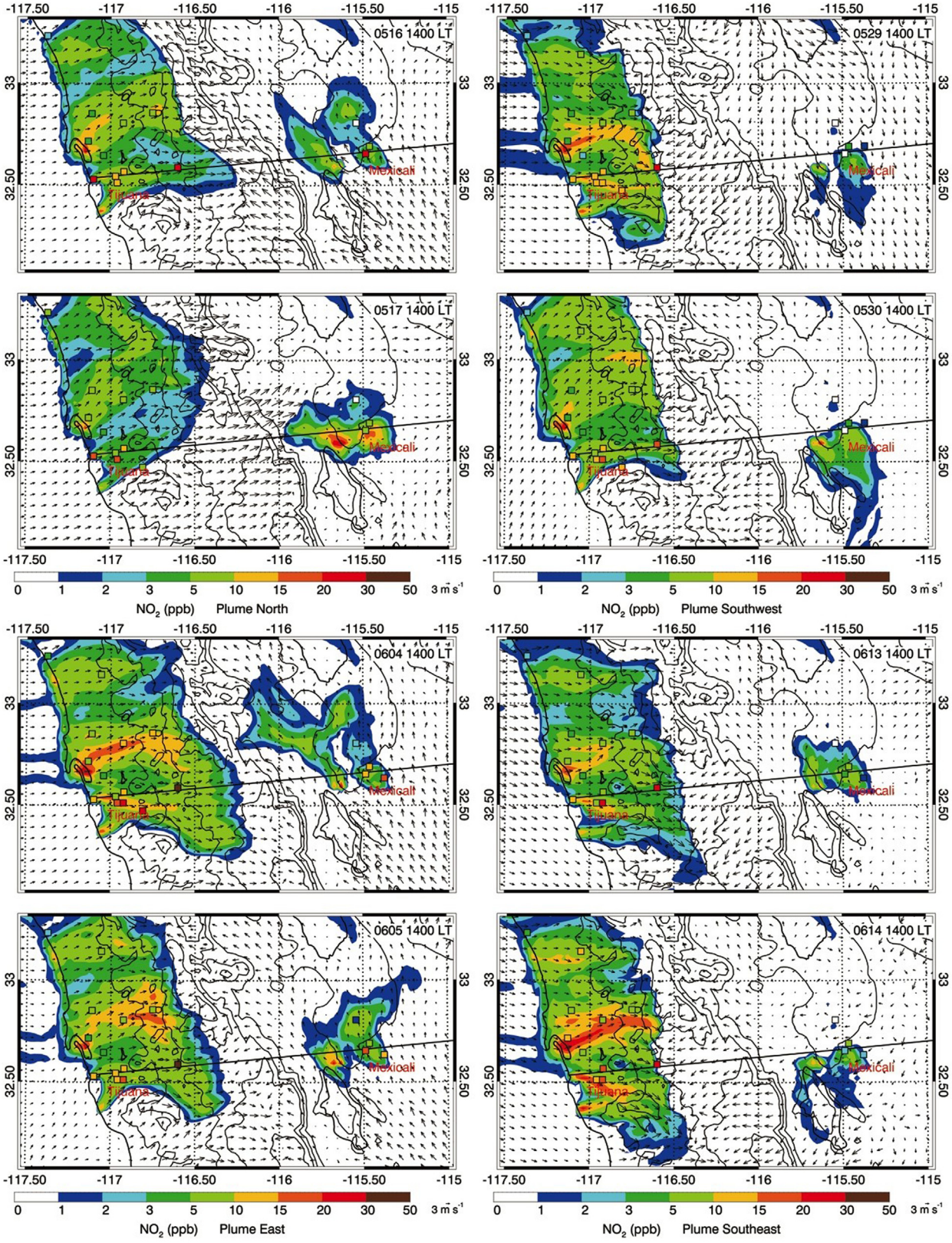

Fig. 6. Same as Fig. 2, but for NO_2.

(defines as O_3(emission control) − O_3(reference)) during the O_3 peak time (defines as 12–1400 LT hereafter). In the urban area and its downwind region, the simulated near-surface O_3 concentrations generally increase by 5–20 ppb, and on June 04, 05 and 14, 2010, the near-surface O_3 concentrations are enhanced by more than 20 ppb in the San Diego downwind region. The response of O_3 change to 50% reduction of NO_x emissions in Calexico–Mexicali is not as significant as that in the San Diego–Tijuana region, and

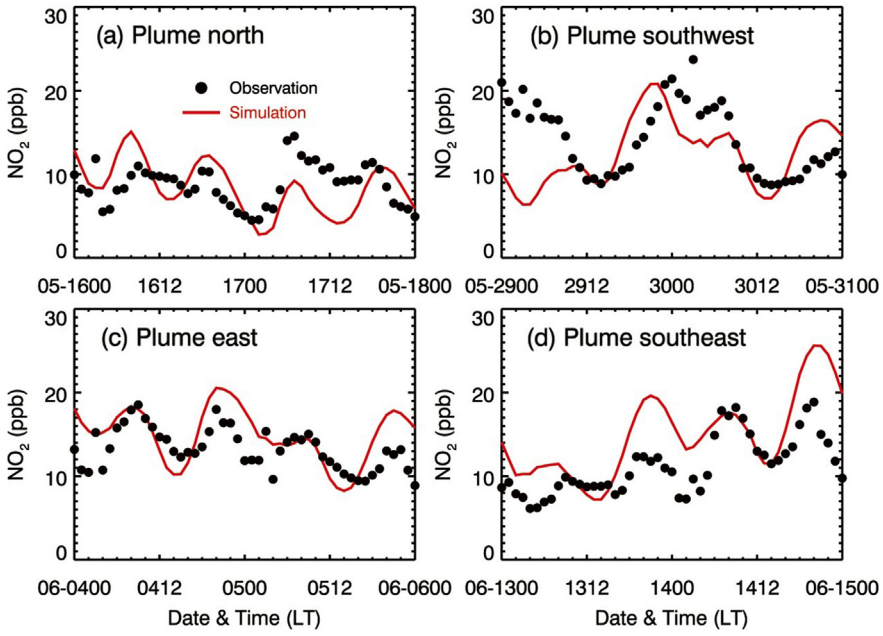

Fig. 7. Same as Fig. 4, but for NO_2 in the San Diego–Tijuana region.

the O_3 concentration change is less than 5 ppb on May 29 and June 14, 2010. When AVOCs emissions are reduced by 50% (Fig. 10), in the San Diego–Tijuana region, the near-surface O_3 concentrations are decreased by 5–20 ppb in the downwind region of urban areas, while the O_3 concentration decrease is generally less than 10 ppb in the Calexico–Mexicali region. Therefore, the sensitivity results show that the O_3 production is VOC-limited in the urban area and its downwind region along the California–Mexico border region.

The ratio of the production rates of hydrogen peroxide and nitric acid (H_2O_2/HNO_3) has been used widely as an indicator for examining VOC–NO_x sensitive photochemistry (Sillman, 1995). A low ratio (less than 0.3) indicates VOC sensitivity, while a high ratio (more than 0.5) indicates NO_x sensitivity. The transition from NO_x to VOC-sensitive chemistry occurs at the ratio between 0.3 and 0.5. Fig. 11 shows the distribution of the averaged H_2O_2/HNO_3 during the O_3 peak time of the four episodes. The regions with the ratio less than 0.3 generally corresponds to those with O_3 increase due to 50% reduction of NO_x emissions (Fig. 9) and those with O_3 decrease due to 50% reduction of AVOCs emissions (Fig. 10). The analyses using H_2O_2/HNO_3 indicator are consistent with the results obtained from sensitivity studies about the VOC-limited for O_3 production in the urban area and its downwind region.

3.3. Contributions of biogenic emissions to O_3 formation

The simulated O_3 patterns (Fig. 2) clearly show that O_3 concentrations increase with the altitude in the afternoon during the four episodes in the San Diego–Tijuana region. Therefore we have classified the observations sites into three types: the low sites with altitude less than 100 m, the middle sites with altitude between 100 and 500 m, and the high sites with altitude more than 500 m (Fig. 1). Fig. 12a presents the observed O_3 daily cycles averaged over the three kinds of sites and during the entire Cal–Mex 2010 campaign. As can be seen, the observed daytime O_3 levels increase with the altitude, from about 40 ppb over the low sites to more than 60 ppb over the high sites in the afternoon. The anthropogenic pollutants emissions are concentrated in the urbanized coastal region and carried inland toward the foothills in the morning. High O_3 concentrations over mountain regions likely result from the photochemical reactions of anthropogenic pollutants during the transport. The local emissions over the mountain region, mainly biogenic emissions, might also contribute to the high O_3 level.

Numerous studies have demonstrated that biogenic emissions play an important role in O_3 formation (e.g., Dreyfus et al., 2002; Steiner et al., 2007). The total impact of biogenic emissions on the O_3 concentration is investigated using the FSA by differentiating two simulations: f_{AB} with both the anthropogenic and biogenic emissions, and f_A with only the anthropogenic emissions. Fig. 13 shows the contribution of near-surface O_3 concentrations during

Table 1
Statistical comparison of simulated and measured O_3 and NO_2 concentrations at monitoring sites during the whole four selected episodes.

Region	Site	O_3			NO_2		
		MB (ppb)	R^2	RMSE (ppb)	MB (ppb)	R^2	RMSE (ppb)
San Diego	SAN01	−7.6	0.41	13.9	5.4	0.17	8.4
	SAN02	−2.6	0.79	7.1	6.5	0.38	8.7
	SAN03	−6.0	0.56	10.8	6.3	0.14	8.8
	SAN04	−1.6	0.32	11.1			
	SAN05	0.90	0.65	8.6			
	SAN06	−4.2	0.58	12.0	−1.8	0.17	5.2
	SAN07	−0.72	0.44	9.3	0.59	0.18	3.0
	SAN08	−14.3	0.33	19.0	16.1	0.14	19.4
	SAN10	−4.2	0.52	10.5			
	SAN11	13.5	0.27	22.0			
	SAN12	1.6	0.47	9.4	−2.0	0.10	8.3
Calexico	IMP01	−0.01	0.65	10.3			
	IMP03	1.4	0.54	11.2			
	IMP04	1.1	0.20	16.9			
	IMP05	1.4	0.55	10.6			
Tijuana	ITT	−6.9	0.50	11.6	6.2	0.12	10.8
	LAM	−3.2	0.61	9.5	2.9	0.24	10.4
	PLA	0.0	0.36	12.0	−9.6	0.31	11.2
	ROS	8.5	0.28	13.8			
	TKT	8.2	0.44	17.2	−18.7	0.19	19.0
	PQM	−1.0	0.49	10.2			
	UTT	8.7	0.49	18.4			
Mexicali	COB	6.3	0.48	14.4			
	ITM	−3.1	0.47	13.8			

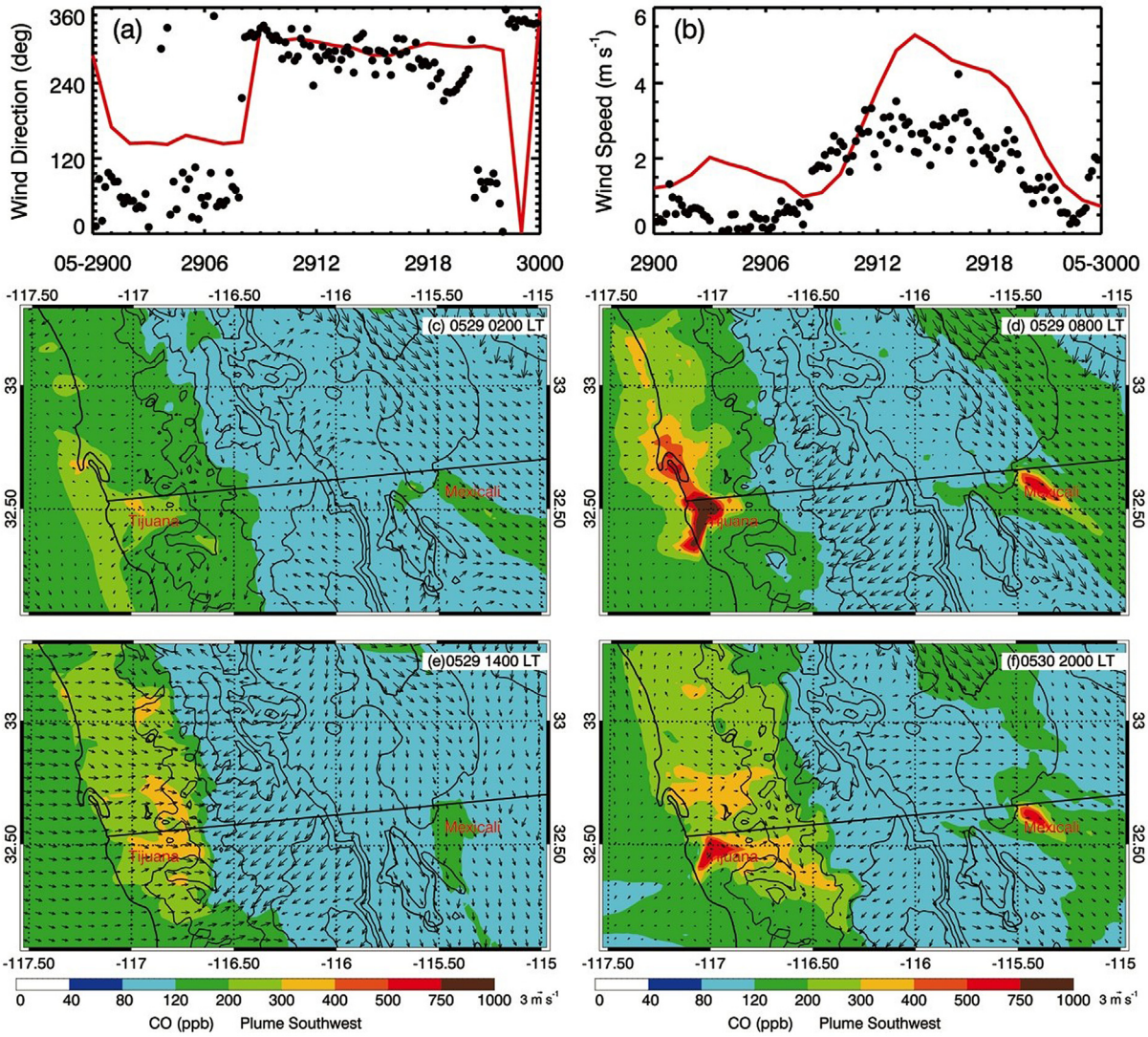

Fig. 8. Simulated vs. observed temporal variations of the near-surface wind (a) direction and (b) speed at PQM, and simulated near-surface winds and CO distributions at (c) 0200, (d) 0800, (e) 1400, and (f) 2000 LT on May 29. Color contour: CO simulations; black arrows: simulated surface winds. (For interpretation of the references to color in this figure legend, the reader is referred to the web version of this article.)

the O_3 peak time from biogenic emissions, i.e. $f_{AB} - f_A$. In San Diego–Tijuana, the biogenic emissions substantially enhance the near-surface O_3 concentrations over the mountain area during the plume east episode, with O_3 increase up to 40 ppb. The enhancement of the near-surface O_3 concentrations is about 5–25 ppb over the mountain area during the plume southwest and southeast episodes. The influence of biogenic emissions on the O_3 concentration is not as remarkable over the mountain area during the plume north episode compared to those during the other three episodes, but the near-surface O_3 concentrations are still increased by up to 3–15 ppb. In the Calexico–Mexicali region, the O_3 enhancement due to biogenic emissions is generally less than 10 ppb, except during the plume east episode with the O_3 increase of over 15 ppb.

Fig. 12b–e show measured and simulated diurnal profiles of near-surface hourly O_3 concentrations averaged over low, middle and high sites during the four episodes. The impact of biogenic emissions on the O_3 level over the low sites is negligible (<2 ppb). The biogenic emissions increase the O_3 concentrations by more than 10 ppb over the middle sites, but are negligible in enhancing O_3 concentrations during the plume north episode. The biogenic emissions enhance O_3 concentrations by more than 30 ppb over high sites, and improve the O_3 simulations against measurements significantly.

3.4. Impacts of trans-boundary transport of pollutants on O_3 level

We use FSA to evaluate the impact of interactions of trans-boundary transport of pollutants from California and Baja California on the O_3 level along the California–Mexico border region. We perform four model simulations: f_{CM} with both the emissions of California and Mexico part, f_C with the emissions of California alone, f_M with the emissions of Mexico part alone, and f_0 without both the emissions of California and Mexico part.

Several studies have indicated that the Mexican emissions have contributed to the O_3 exceedances in Southern California (Wang et al., 2009; Huang et al., 2011). Fig. 14 presents the averaged peak time O_3 contribution distribution from the Baja California emissions ($f_{CM} - f_C$). Firstly, except in the mountain area near the California–Mexico border, the Baja California

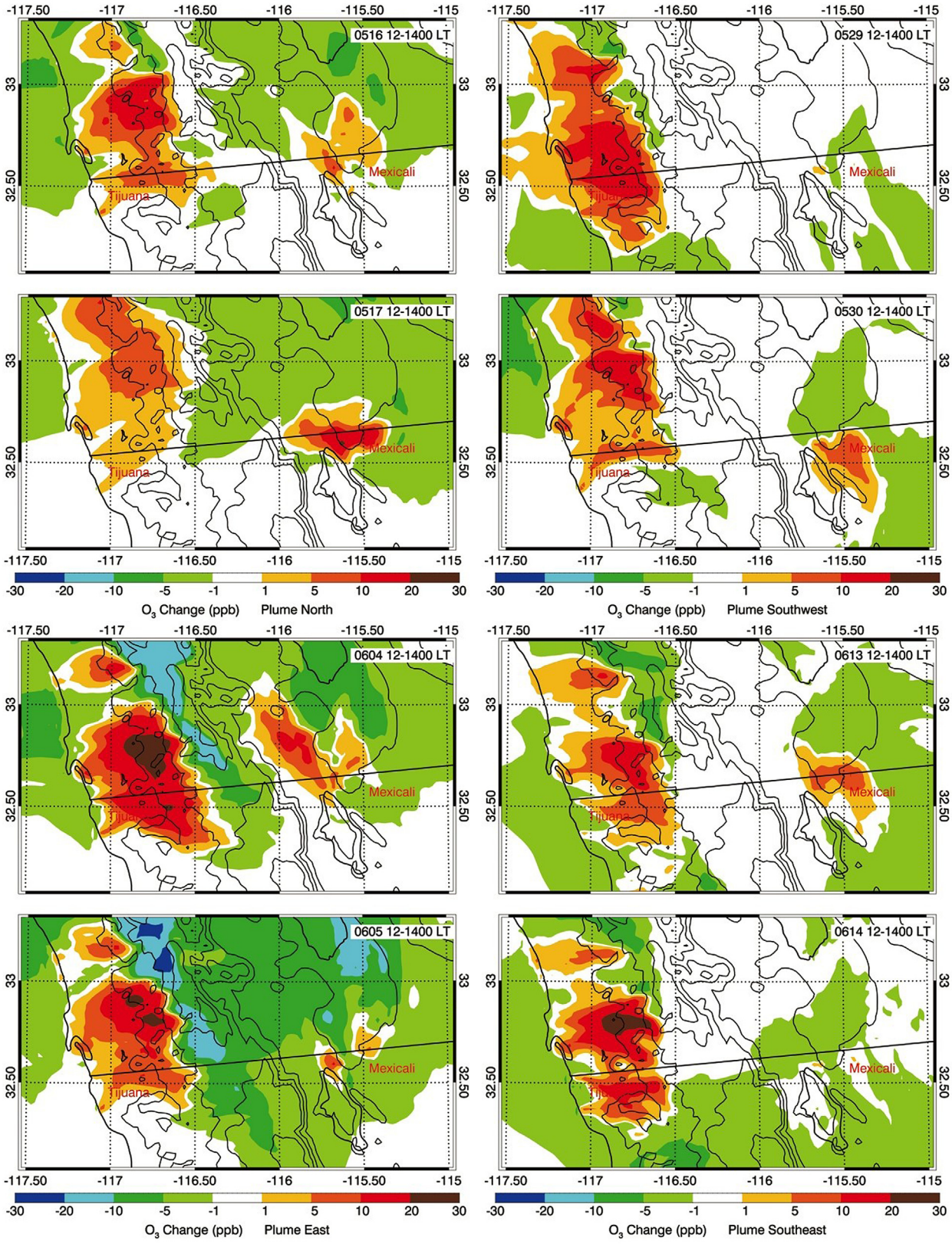

Fig. 9. Percentage change of O_3 concentrations in the bottom model layer, averaged from 1200 to 1400 LT over the four selected episodes due to a 50% reduction of NO_x emissions.

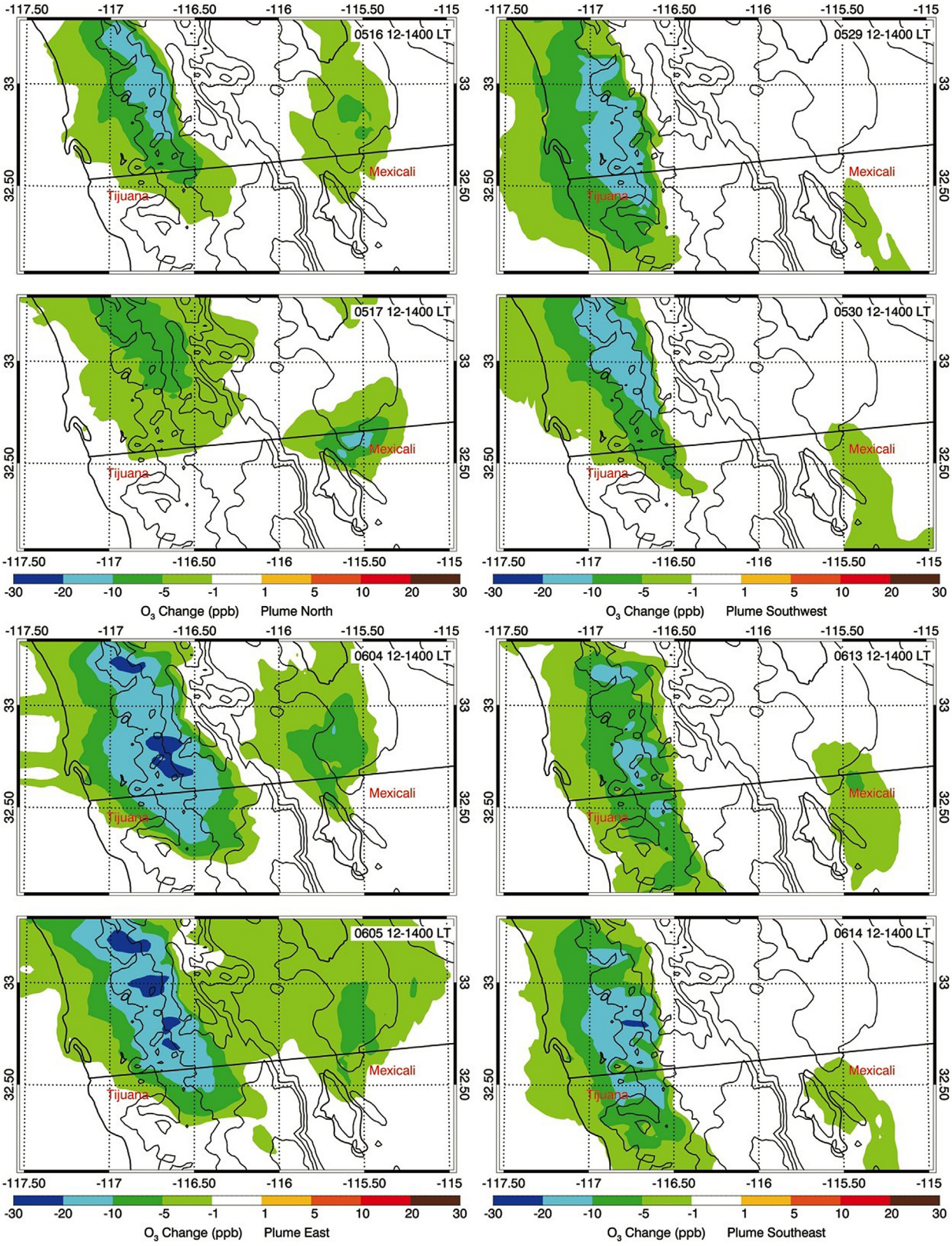

Fig. 10. Same as Fig. 9, but for 50% reduction of AVOCs emissions.

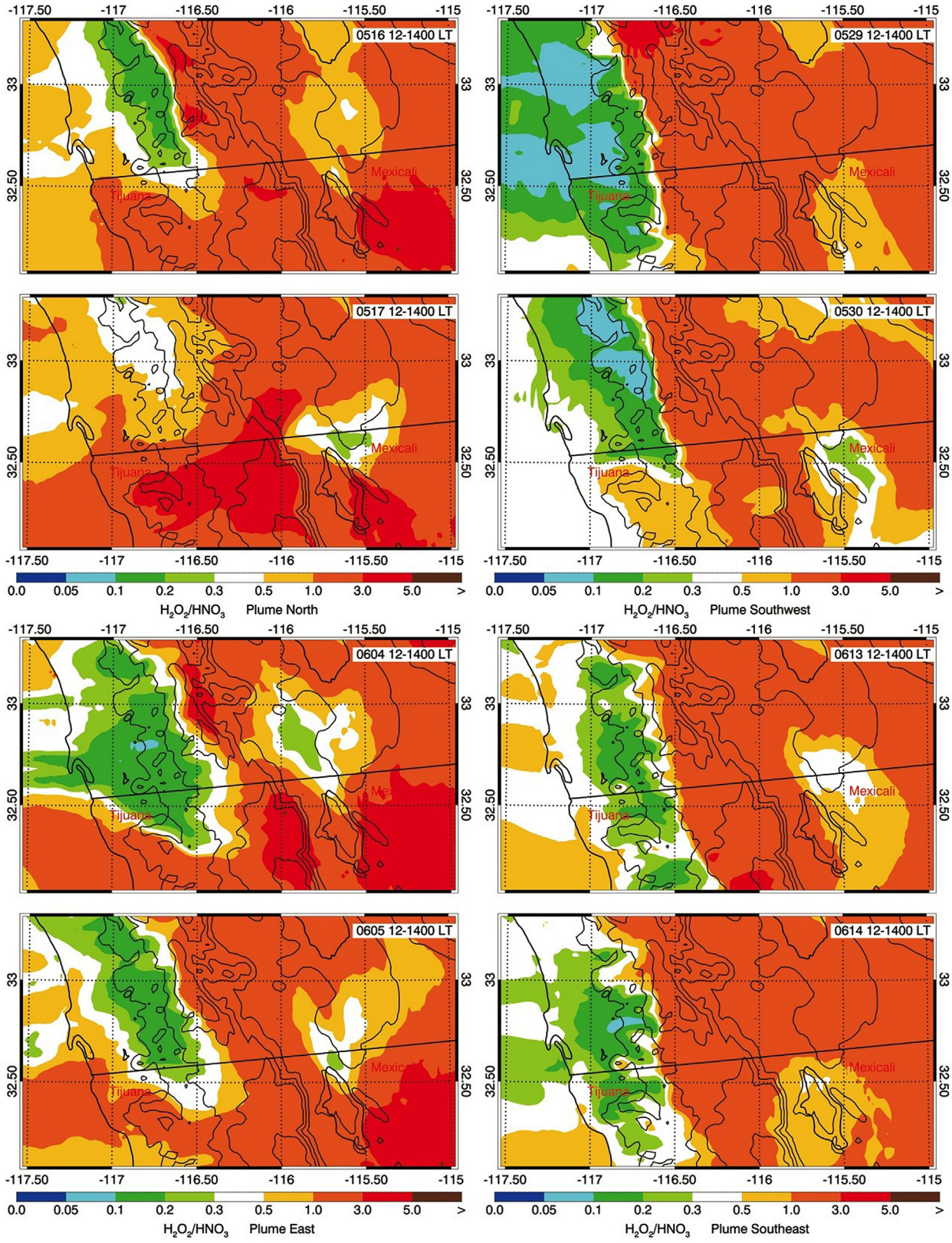

Fig. 11. Ratio of H_2O_2/HNO_3 in the bottom model layer, averaged from 1200 to 1400 LT over the four selected episodes.

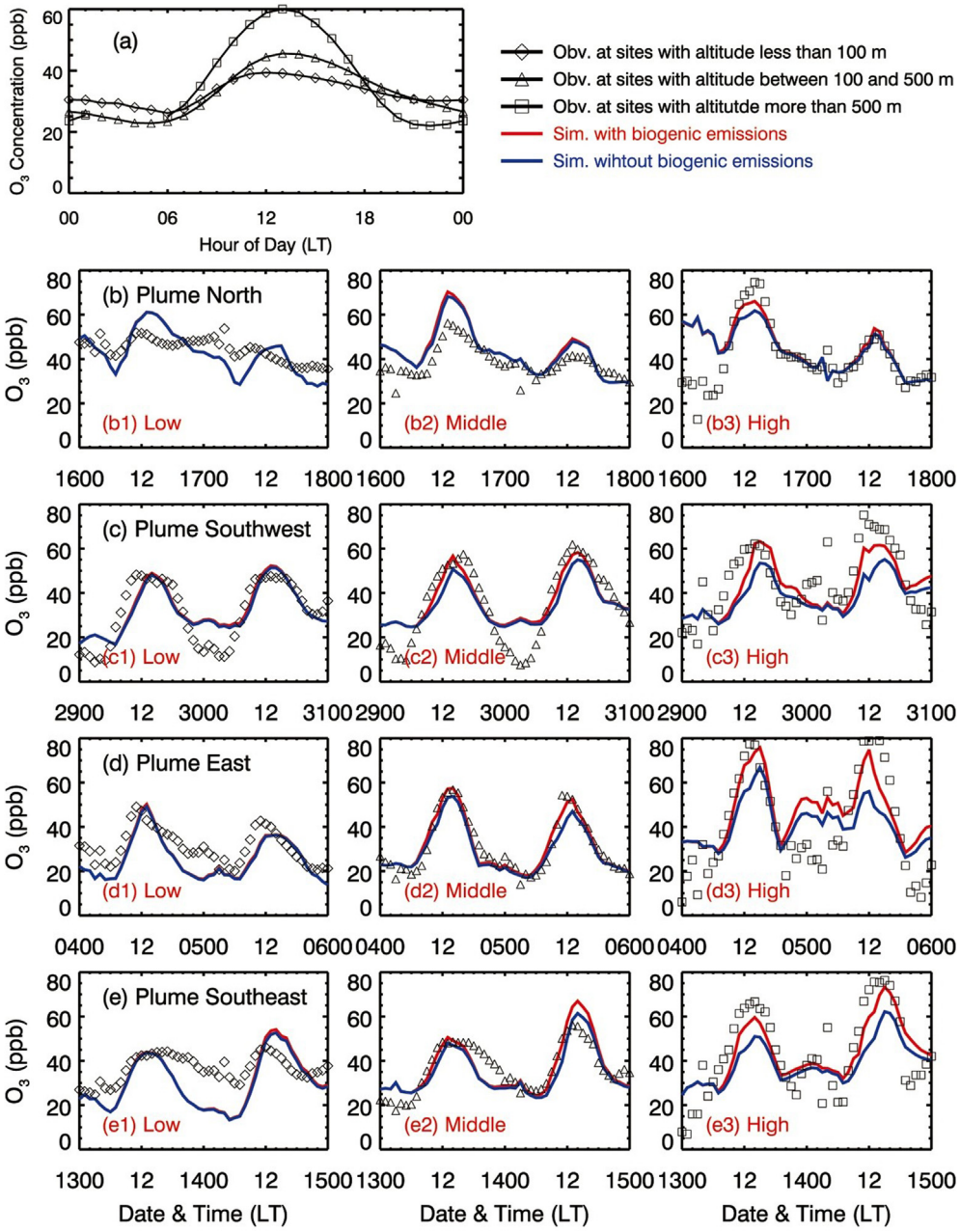

Fig. 12. (a) Observed O_3 daily cycles averaged during the entire Cal–Mex 2010 field campaign, and (b)–(e) comparisons of measured vs. simulated diurnal profiles of near-surface hourly O_3 averaged over the low, middle and high sites in the San Diego–Tijuana region during the four selected episodes.

emissions do not substantially impact the O_3 level in San Diego, with the O_3 change ranging from −5 to +5 ppb. Secondly, when the south wind components are weak in the San Diego–Tijuana region, the emissions from Baja California cannot be transported to Southern California efficiently and the O_3 contribution to the San Diego region is minor, such as on May 29, June 13 and 14. During the plume southwest and southeast episodes when the south wind components are not weak in the Calexico–Mexicali region, the Baja California emissions affect considerably the near surface O_3 level, with the O_3 contribution of up to 20 ppb. Table 2 provides the averaged peak time O_3 and NO_2 contribution due to the Baja California emissions at monitoring stations in the San Diego and Calexico regions. In San Diego, the O_3 enhancement due to the Baja California emissions is less than 2 ppb at monitoring stations, indicating that the O_3 exceedances in the region is principally caused by local emissions. Furthermore, the Baja California emissions increase the NO_2 concentrations at each monitoring station by up to 5.4 ppb. In Calexico, during the plume east, the O_3 level at monitoring stations is enhanced by the Baja California emissions by 2.6–12.7 ppb, showing that the Mexico emissions have potentials to contribute to the O_3 exceedances in the region.

Fig. 15 shows the distribution of near-surface O_3 change due to the interactions of trans-boundary transport of pollutants between California and Baja California (f'_{CM}) at 1400 LT during the four episodes. Generally, the interactions of emitted pollutants from California and Baja California decrease the near-surface O_3 concentrations along the border region. The impact of the

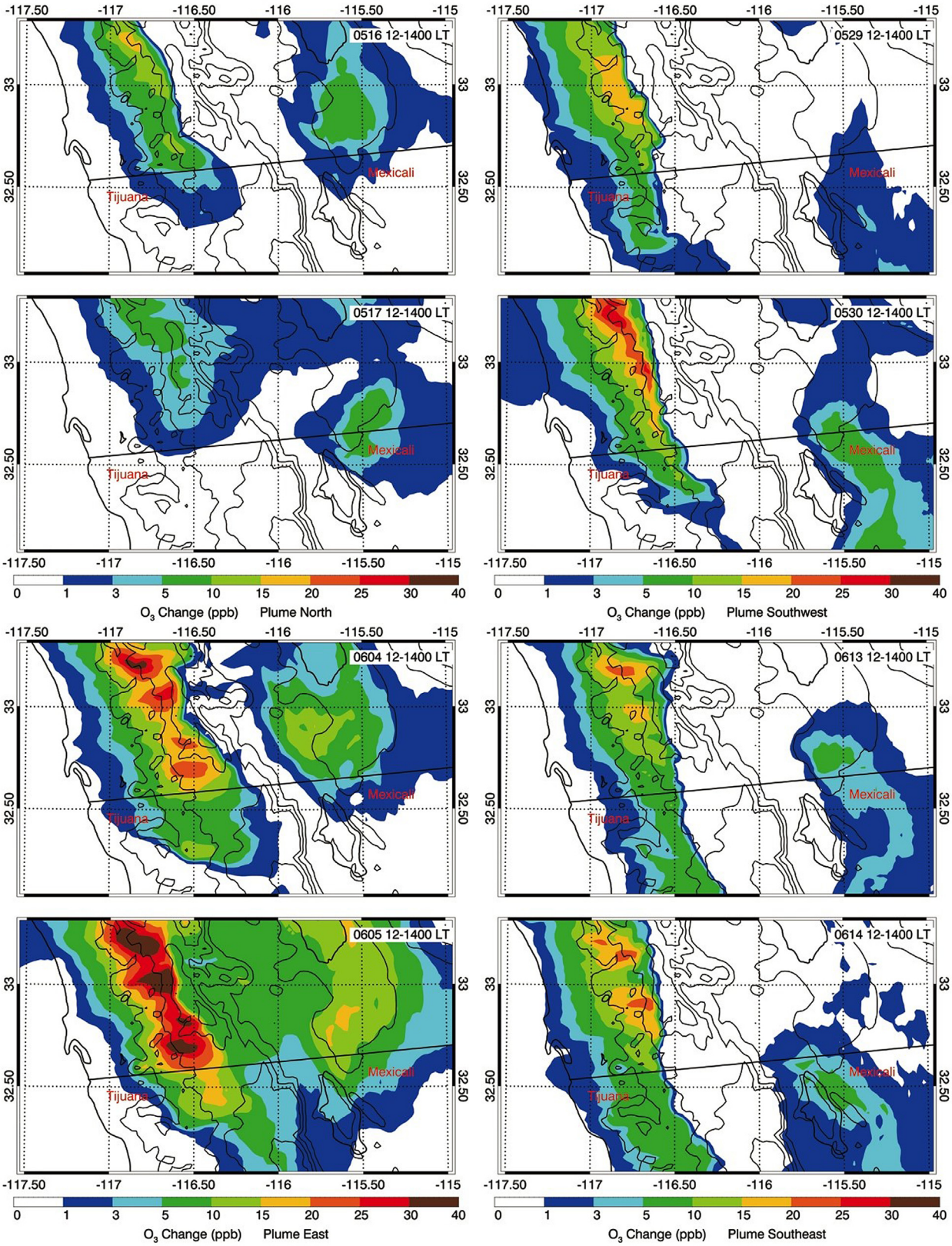

Fig. 13. Contributions of biogenic emissions to near-surface O_3 concentrations averaged from 1200 to 1400 LT over the four selected episodes.

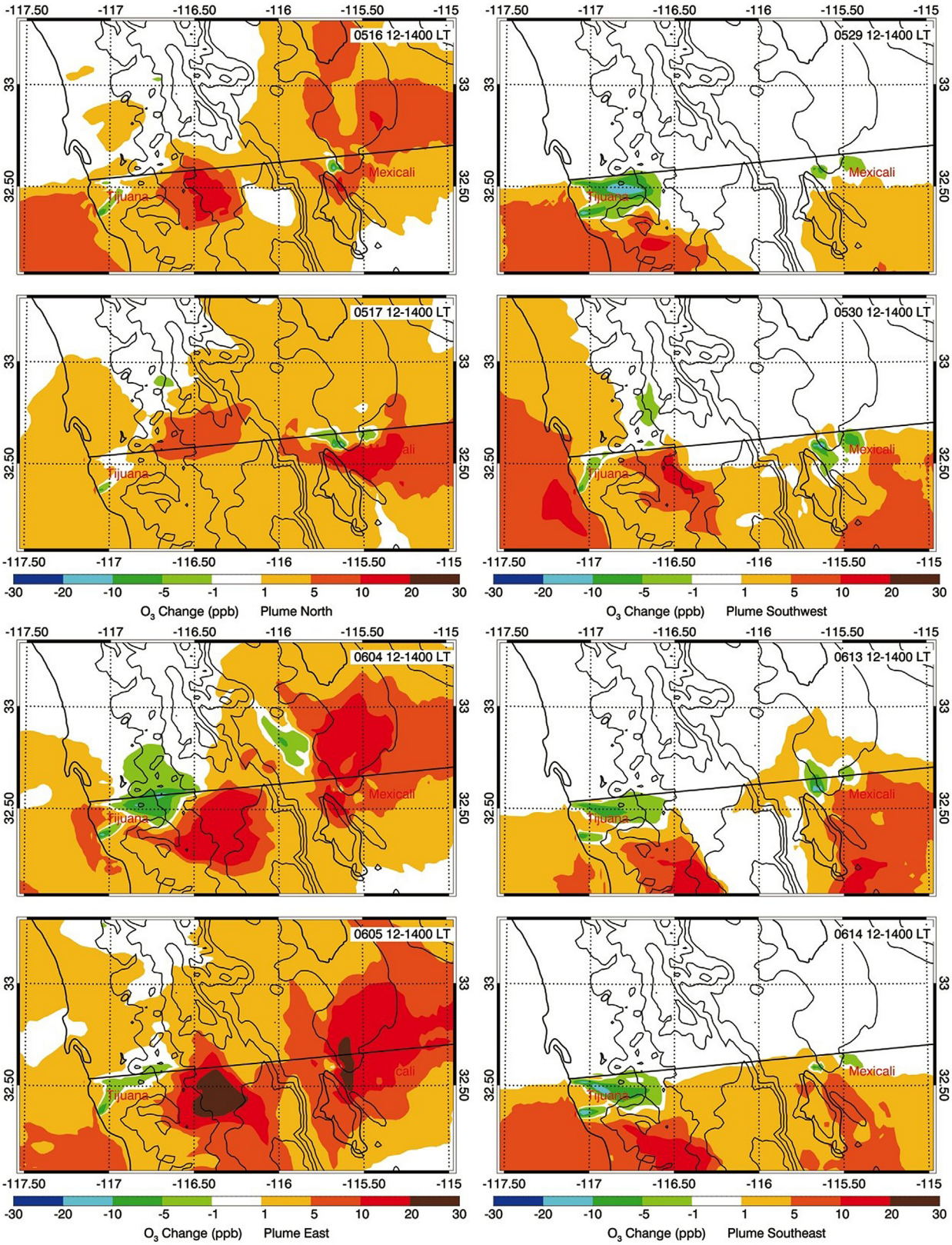

Fig. 14. Contributions of Baja California emissions to near-surface O_3 concentrations averaged from 1200 to 1400 LT over the four selected episodes.

Table 2
O_3 and NO_2 contributions from Baja California emissions at monitoring sites in the San Diego and Calexico regions, averaged from 1200 to 1400 LT during the four selected episodes.

Plume	North		Southwest		East		Southeast	
Site	O_3 (ppb)	NO_2 (ppb)	O_3 (ppb)	NO_2 (ppb)	O_3 (ppb)	NO_2 (ppb)	O_3 (ppb)	NO_2 (ppb)
SAN01	+1.6	+0.1	+1.8	+0.1	−0.4	+0.7	−0.0	+0.0
SAN02	+1.0	+1.0	+0.3	+0.6	+0.1	+0.8	−0.1	+0.0
SAN03	+1.1	+0.3	+1.1	+0.2	+0.7	+0.4	−0.0	+0.0
SAN04	+1.0	+0.0	+1.7	+0.1	+0.9	+0.1	−0.0	+0.0
SAN05	−0.1	+0.2	−0.2	+0.2	+0.1	+0.3	−0.0	+0.0
SAN06	−1.0	+1.4	−1.0	+0.6	+0.3	+0.6	−0.0	+0.0
SAN07	+0.1	+0.1	+0.9	+0.1	+0.4	+0.3	+0.0	+0.0
SAN08	+1.4	+0.2	+1.6	+0.3	+0.3	+0.4	−0.0	+0.0
SAN10	+1.1	+0.3	+1.1	+0.2	+0.8	+0.4	−0.0	+0.0
SAN11	−0.2	+0.2	−0.1	+0.1	−0.5	+0.2	−0.0	+0.0
SAN12	+0.5	+4.5	−1.0	+5.2	−2.8	+5.4	−0.1	+1.0
IMP01	−0.5	+5.2	+0.1	+0.1	+6.9	+8.1	−2.0	+2.4
IMP02	+5.3	+3.1	+0.2	+0.2	+12.7	+3.6	+0.1	+1.5
IMP03	−1.2	+2.5	+0.2	+0.0	+7.5	+2.8	+0.7	+0.1
IMP04	+3.2	+0.2	+0.1	+0.0	+2.6	+0.1	+0.3	+0.0
IMP05	+4.3	+0.2	−0.0	+0.0	+3.7	+0.1	+0.0	+0.0

interaction is most remarkable during the plume east episode and the near surface O_3 concentrations are reduced by up to 30 ppb. During the plume north and east episodes, the interactions of emissions from Baja California with those from California decrease considerably the surface O_3 level in San Diego and Calexico regions. Near-surface O_3 concentrations are increased mainly over the sea in the Mexico part due to the trans-boundary emission interactions, with the O_3 enhancement of less than 10 ppb. When the model underestimates the observed O_3 concentrations in Calexico–Mexicali during the plume southwest and southeast episodes, the impact of the emission interactions is generally not significant, which needs to be further investigated.

Fig. 16 provides the temporal variation of the averaged contributions to near-surface O_3 concentrations from pure California emissions ($f_C^{'}$), pure Baja California emissions ($f_M^{'}$), and the interactions of both emissions ($f_{CM}^{'}$) during the four episodes in the four regions defined in Fig. 1: San Diego, Tijuana, Calexico, Mexicali and their surrounding areas. In San Diego and surrounding area, the local emissions dominate the daytime O_3 level, with contributions of more than 30 ppb (Fig. 16a). The Baja California emissions (mainly from Tijuana and the surrounding area) also enhance the daytime O_3 level in the region by up to 5 ppb. However, the O_3 formation is a complicated nonlinear process, not only depending on the absolute levels of precursors, but also on their relative abundance (Lin et al., 1988). When the O_3 precursors emitted from Baja California are transported to San Diego and the surrounding area and mixed with the local emissions, the VOCs and NO_x levels in the mixed emissions are enhanced, but the VOCs/NO_x ratio is also altered, causing the formed O_3 concentration unequal to the simple linear summation of O_3 contributions from the local ($f_C^{'}$) and Baja California ($f_M^{'}$) emissions. The O_3 contribution from the interaction of California and Baja California emissions ($f_{CM}^{'}$) is the difference between the O_3 formed from the mixed emissions and the summation of O_3 contributions from each emission. Considering that the O_3 production is VOC-limited in the urban areas of San Diego and Tijuana and their downwind regions, $f_{CM}^{'}$ is subject to be negative (Lin et al., 1988). In Fig. 16a, the interactions of emissions from California and Baja California decrease daytime O_3 by several ppb in the San Diego and the surrounding region, counteracting the O_3 enhancement from pure Baja California emissions, indicating that the Baja California emissions play a minor role in O_3 formation during daytime. In Tijuana and the surrounding area, the O_3 increase from California emissions substantially exceed the O_3 decrease from the daytime emission interactions during the plume southwest and southeast, showing that the California emissions have important contributions to the daytime O_3 level in the area. However, the Baja California emissions remarkably enhance the daytime O_3 level in the Calexico and surrounding area during the plume north and east episodes. In Mexicali and the surrounding area, the impact of the California emissions on the O_3 level is unimportant.

Fig. 17 provides the temporal variation of the averaged contributions to near-surface O_3 concentrations along the California–Mexico border region (within 40 km to the border) from pure California emissions, pure Baja California emissions, and the interactions of both emissions during the four episodes. The contribution from pure California emissions to the O_3 level along the California–Mexico border region is comparable to those from pure Baja California during the plume north episode, and O_3 concentrations are increased by several ppb during the afternoon and decreased by less than 2 ppb during nighttime on average. During the other three episodes, the pure California emissions contribute more O_3 than the pure Baja California emissions during daytime, particularly during the plume southeast episode, indicating that the pure California emissions play a more important role than the pure Baja California emissions in the high O_3 level along the border region. However, the interactions of pollutants emitted from California and Baja California decrease the O_3 level along the border region by less than 4 ppb during daytime due to the nonlinear process of the O_3 formation and the VOC-limited regime for O_3 production in the urban areas of the sister cities of San Diego–Tijuana and Calexico–Mexicali and their downwind regions.

4. Conclusions

In the present study, four two-day episodes during the Cal–Mex 2010 field campaign are simulated along the California–Mexico border region using the WRF-CHEM model to verify the O_3 formation, including May 15–16 (plume north), May 29–30 (plume southwest), June 4–5 (plume east), and June 13–14 (plume southeast). The model reproduces well the O_3 distribution and variation in the San Diego–Tijuana region compared to the observations, but in the Calexico–Mexicali region, the model underestimate the observations during the plume southwest and southeast episodes, which is perhaps caused by the uncertainties of simulated meteorological fields in the morning. Additionally, although the model generally simulates reasonably well the pattern and variation of the observed NO_2 concentrations during daytime in San Diego–Tijuana region, it still has difficulties in replicating the measurements during nighttime. The sensitivity studies through reducing the AVOCs and NO_x emissions by 50% show that O_3 production is generally VOC-limited in the urban area and its downwind region along the border region.

In San Diego–Tijuana, the simulated O_3 concentrations increase with altitude, consistent with the surface and aircraft measurements. The morning anthropogenic precursor emissions in the urbanized coastal region are transported inland by the sea breeze and mixed with biogenic emissions during the transport, causing high O_3 level over the mountain regions. Biogenic emissions play an important role in the O_3 formation over the mountain region, with the O_3 contribution of up to 40 ppb during peak time. In Calexico–Mexicali, the biogenic emissions generally increase the O_3 concentrations by less than 10 ppb, except during the plume east episode, with the O_3 enhancement of over 15 ppb.

The FSA is used to investigate the influence of interactions of trans-boundary transport of pollutants between California and Baja

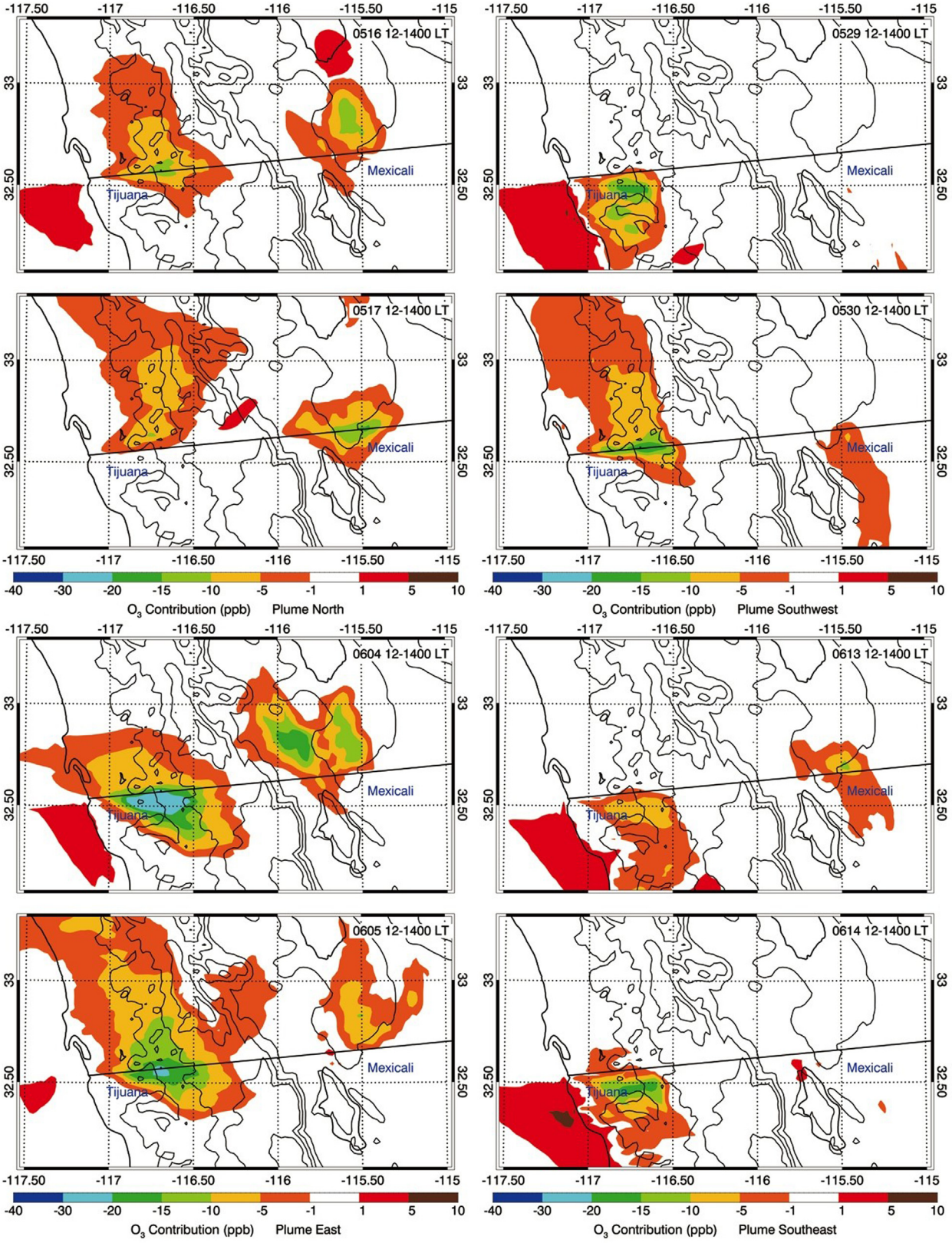

Fig. 15. Distribution of contribution of the near-surface O_3 concentration from the interactions of trans-boundary transport of emissions from California and Baja California averaged from 1200 to 1400 LT over the four selected episodes. The interactions are obtained from FSA using four model runs: f_{CM} with both the emissions of California and Baja California, f_C with the emissions of California alone, f_M with the emissions of Baja California alone, and f_0 without both the emissions, and defined as $f_{CM} + f_0 - f_c - f_M$.

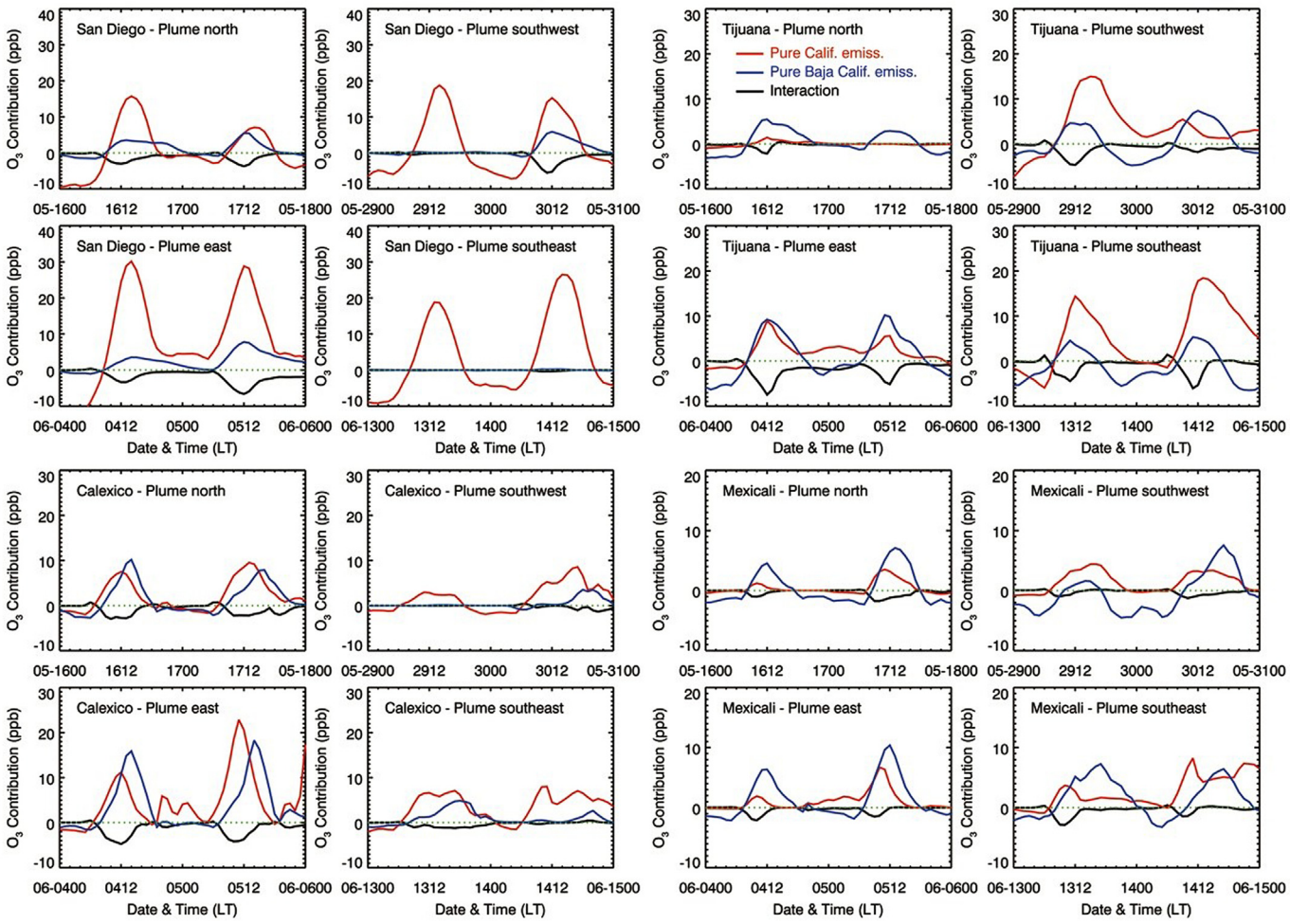

Fig. 16. Temporal variation of the averaged contributions to the near-surface O_3 concentration from pure California emissions (red line, defined as $f_C - f_0$), pure Baja California emissions (blue line, defined as $f_M - f_0$), and the interactions (black line, defined as $f_{CM} + f_0 - f_c - f_M$) in the San Diego, Tijuana, Calexico, and Mexicali and their surrounding areas during the four selected episodes. Definitions of f_{CM}, f_C, f_M, and f_0 can be found in Fig. 15. (For interpretation of the references to color in this figure legend, the reader is referred to the web version of this article.)

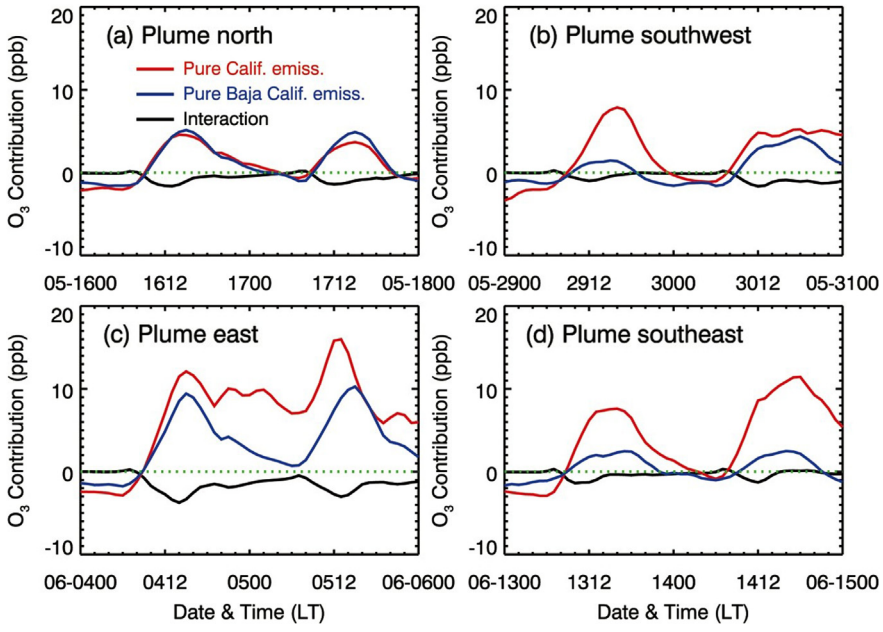

Fig. 17. Same as Fig. 16, but for along the California–Mexico border region (within 40 km to the California–Mexico border).

California on the O_3 level along the border region. Generally, the interactions of emissions from California and Baja California reduce the near surface O_3 concentrations along the border region by up to 40 ppb during the O_3 peak time. The averaged near-surface O_3 reduction due to the interactions in the sister cities of San Diego–Tijuana and Calexico–Mexicali is up to 7 ppb during daytime. The emissions from Baja California play a minor role in the O_3 level in the San Diego and surrounding area due to the nonlinear properties of O_3 formation and do not appear to contribute to the O_3 exceedances in the region. However, California emissions contribute considerably to the O_3 level in Tijuana and the surrounding area. Moreover, Baja California emissions can potentially cause the O_3 exceedances in Calexico and surrounding area. On average, O_3 reduction due to the interactions within 40 km to the California–Mexico border is about 2–4 ppb in the afternoon. Additionally, the emissions from California contribute more O_3 than those from Baja California along the border region in general.

It is worth noting that, although the model reasonably reproduces the patterns and variations of observed O_3 and NO_2 concentrations during daytime, the model still has difficulties in nighttime simulations. The discrepancies between simulations and observations are likely due to the uncertainties in the emission inventory (which needs further validation in future studies) and the meteorological fields (which significantly influence the O_3 and NO_2 simulations in the model). The California–Mexico border region is frequently influenced by sea breeze. Although the experience with sea-breeze simulations has extended over many decades, it is still difficult for current numerical weather prediction models, even in research mode, to reproduce the location, timing, depth, and intensity of the sea-breeze front (Banta et al., 2005). Further studies need to be performed to improve the meteorological field simulations in the California–Mexico border region for the evaluation of the O_3 formation.

Acknowledgments

This work was supported by the US National Science Foundation Atmospheric Chemistry Program (Award 1009393), Environmental Protection Agency, California Air Resources Board, National Institute of Ecology of Mexico, and the National Natural Science Foundation of China (no. 41275153, 41275101). Guohui Li is also supported by the "Hundred Talents Program" of the Chinese Academy of Sciences. Acknowledgment is also made to the National Center for Atmospheric Research, which is sponsored by the National Science Foundation, for the computing time used in this research.

References

Banta, R.M., Senff, C.J., Ryerson, T.B., Nielsen-Gammon, J., Darby, L.S., Alvarez, R.J., Sandberg, S.P., Williams, E.J., Trainer, M., 2005. A bad air day in Houston. Bull. Am. Meteorol. Soc. 86, 657–669.

Bei, N., de Foy, B., Lei, W., Zavala, M., Molina, L.T., 2008. Using 3DVAR data assimilation system to improve ozone simulations in the Mexico City basin. Atmos. Chem. Phys. 8, 7353–7366.

Bei, N., Lei, W., Zavala, M., Molina, L.T., 2010. Ozone predictabilities due to meteorological uncertainties in Mexico City Basin using ensemble forecasts. Atmos. Chem. Phys. 10, 6295–6309.

Bei, N., Li, G., Molina, L.T., 2012. Uncertainties in SOA simulations due to meteorological uncertainties in Mexico City during MILAGRO-2006 field campaign. Atmos. Chem. Phys. 12, 11295–11308.

Bei, N., Li, G., Zavala, M., Barrera, H., Torres, R., Grutter, M., Gutiérrez, W., García, M., Ruiz-Suarez, L.G., Ortinez, A., Guitierrez, Y., Alvarado, C., Flores, I., Molina, L.T., 2013. Meteorological overview and plume transport patterns during Cal-Mex 2010. Atmos. Environ. 70, 477–489.

Bigler-Engler, V., Brown, H.W., 1995. Analysis of an ozone episode during the San Diego air quality study: the significance of transport. J. Appl. Meteorol. 34, 1863–1876.

Chameides, W.L., Lindsay, R.W., Richardson, J., Kiang, C.S., 1988. The role of biogenic hydrocarbons in urban photochemical smog: Atlantic as a case study. Science 241, 1473–1475.

Chen, F., Dudia, J., 2001. Coupling an advanced land-surface/hydrology model with the Penn State/NCARMM5modelingsystem. Part I: model description and implementation. Mon. Wea. Rev. 129, 569–585.

Dreyfus, G.B., Schade, G.W., Goldstein, A.H., 2002. Observational constraints on the contribution of isoprene oxidation to ozone production on the western slope of the Sierra Nevada, California. J. Geophys. Res. 107, 4367. http://dx.doi.org/10.1029/2001JD001490.

Dudia, J., 1989. Numerical study of convection observed during the winter monsoon experiment using a mesoscale two-dimensional model. J. Atmos. Sci. 46, 3077–3107.

Grell, G.A., Peckham, S.E., Schmitz, R., McKeen, S.A., Wilczak, J., Eder, B., 2005. Fully coupled "online" chemistry within the WRF model. Atmos. Environ. 39, 6957–6975.

Guenther, A., Karl, T., Harley, P., Wiedinmyer, C., Palmer, P.I., Geron, C., 2006. Estimates of global terrestrial isoprene emissions using MEGAN (Model of Emissions of Gases and Aerosols from Nature). Atmos. Chem. Phys. 6, 3181–3210.

Huang, M., Carmichael, G.R., Spak, S.N., Adhikary, B., Kulkarni, S., et al., 2011. Multiscale modeling study of the source contributions to near-surface ozone and sulfur oxides levels over California during the ARCTAS-CARB period. Atmos. Chem. Phys. 11, 3173–3194.

Li, G., Zhang, R., Fan, J., Tie, X., 2007. Impacts of biogenic emissions on photochemical ozone production in Houston, Texas. J. Geophys. Res. 112, D10309. http://dx.doi.org/10.1029/2006JD007924.

Li, G., Lei, W., Zavala, M., Volkamer, R., Dusanter, S., Stevens, P., Molina, L.T., 2010. Impacts of HONO sources on the photochemistry in Mexico City during the MCMA-2006/MILAGO Campaign. Atmos. Chem. Phys. 10, 6551–6567.

Li, G., Zavala, M., Lei, W., Tsimpidi, A.P., Karydis, V.A., Pandis, S.N., Canagaratna, M.R., Molina, L.T., 2011a. Simulations of organic aerosol concentrations in Mexico City using the WRF-CHEM model during the MCMA-2006/MILAGRO campaign. Atmos. Chem. Phys. 11, 3789–3809.

Li, G., Bei, N., Tie, X., Molina, L.T., 2011b. Aerosol effects on the photochemistry in Mexico City during MCMA-2006/MILAGRO campaign. Atmos. Chem. Phys. 11, 5169–5182.

Li, G., Lei, W., Bei, N., Molina, L.T., 2012. Contribution of garbage burning to chloride and $PM_{2.5}$ in Mexico City. Atmos. Chem. Phys. 12, 8751–8761.

Luria, M., Tanner, R.L., Valente, R.J., Bairai, S.T., Koracin, D., Gertler, A.W., 2005. Local and transported pollution over San Diego, California. Atmos. Environ. 39, 6765–6776.

Lin, X., Trainer, M., Liu, S.C., 1988. On the nonlinearity of the tropospheric ozone. J. Geophys. Res. 93, 15879–15888.

Lin, Y.-L., Farley, R.D., Orville, H.D., 1983. Bulk parameterization of the snow field in a cloud model. J. Appl. Meteorol. 22, 1065–1092.

Mlawer, E.J., Taubman, S.J., Brown, P.D., Iacono, M.J., Clough, S.A., 1997. Radiative transfer for inhomogeneous atmosphere: RRTM, a validated correlated-k model for the long-wave. J. Geophys. Res. 102 (D14), 16663–16682.

Noh, Y., Cheon, W.G., Raasch, S., 2001. The improvement of the K-profile model for the PBL using LES. In: Preprints, Int. Workshop of Next Generation NWP Models, Seoul, South Korea. Laboratory for Atmospheric Modeling Research, pp. 65–66.

Osthoff, H.D., Roberts, J.M., Ravishankara, A.R., Williams, E.J., Lerner, B.M., et al., 2008. High levels of nitryl chloride in the polluted subtropical marine boundary layer. Nat. Geosci. 1, 324–328.

Shi, C., Fernando, H.J.S., Yang, J., 2009. Contributors to ozone episodes in three U.S./Mexico border twin-cities. Sci. Total Environ. 407, 5128–5138.

Sillman, S., 1995. The use of NO_y, H_2O_2 and HNO_3 as indicators for O_3-NO_x-VOC sensitivity in urban locations. J. Geophys. Res. 100, 14,175–14,188.

Stein, D., Alpert, P., 1993. Factor separation in numerical simulations. J. Atmos. Sci. 50, 2107–2115.

Steiner, A.L., Tonse, S., Cohen, R.C., Goldstein, A.H., Harley, R.A., 2007. iBiogenic 2-methyl-3-buten-2-ol increases regional ozone and HO_x sources. Geophys. Res. Lett. 34, L15806. http://dx.doi.org/10.1029/2007GL030802.

U.S. Environmental Protection Agency, 2008. U.S.-Mexico Environmental Program: Border 2012 A Mid Course Refinement (2008–2012). EPA-909-R-08–003. Accessed at: http://www.epa.gov/usmexicoborder/docs/B2012_New_Objectives.pdf.

Wang, H., Jacob, D.J., Sager, P.L., Streets, D.J., Park, R.J., Gilliland, A.B., van Donkelaar, A., 2009. Surface ozone background in the United States: Canadian and Mexican pollution influences. Atmos. Environ. 43, 1310–1319.

Wang, J., Ge, C., Yang, Z., Hyer, E.J., Reid, J.S., Chew, B.N., Mahmud, M., Zhang, Y., Zhang, M., 2013. Mesoscale modeling of smoke transport over the Southeast Asian Maritime Continent: interplay of sea breeze, trade wind, typhoon, and topography. Atmos. Res. 122, 486–503.